

# Rheological Properties of Liquid Crystalline Solutions of Ethyl Celluloses with Different Molecular Weight in *m*-Cresol

SHINICHI SUTO, MASAHIKO OHSHIRO, WATARU NISHIBORI, HISASHI TOMITA, and MIKIO KARASAWA,  
*Department of Polymer Chemistry, Faculty of Engineering, Yamagata University, Jonan 4-3-16, Yonezawa, Yamagata, 992, Japan*

## Synopsis

Steady-state shear rheological properties of liquid crystalline solutions of four ethyl celluloses (ECs) were determined at a low shear rate ( $1 \text{ s}^{-1}$ ) and at relatively high shear rates by using two rheometers (cone-plate and capillary types), and were compared with those of liquid crystalline hydroxypropyl cellulose (HPC). The effect of molecular weight (MW) on the viscoelastic behavior was also determined. The viscometric behavior of EC solutions was similar to that of HPC solutions: (1) with respect to temperature, the shear viscosity ( $\eta$ ) at shear rate of  $1 \text{ s}^{-1}$  exhibited a minimum ( $\eta_{\min}$ ) and a maximum ( $\eta_{\max}$ ), and the concentration-temperature superposition for  $\eta$  could be applied; (2) the behavior of  $\eta$  at relatively high shear rates as a function of shear rate or polymer concentration was typical of lyotropic liquid crystals. The MW dependence of  $\eta_{\min}$  was greater than that of  $\eta_{\max}$  for EC solutions. The behavior of the elastic parameters such as Bagley correction factor ( $\nu$ ), entrance pressure drop ( $\Delta P_{\text{ent}}$ ), and die swell ( $B$ ) at relatively high shear rates for EC solutions was essentially similar to that for HPC solutions: (1) the shear rate or stress dependence of the elastic parameters was greatly dependent on whether the polymer solution was in a single phase or biphasic; (2) with respect to concentration the elastic parameters showed a maximum and a minimum and the maximum or minimum point for each parameter was not always identical to each other.  $\eta$  for the isotropic or fully anisotropic solutions at a given concentration ( $C$ ) increased, whereas  $\eta$  for the solutions in the vicinity of the biphasic region showed a minimum, with respect to MW. The slope of  $\eta$  at a given shear rate vs.  $C\bar{M}_w$  depended on shear rate, and this slope for the isotropic solutions appeared to be greater than that for fully anisotropic solutions.  $\Delta P_{\text{ent}}$  and  $\nu$  at a given concentration showed either a monotonical increase or a maximum or minimum with MW, and this behavior was not fully consistent with that of  $\eta$ .  $B$  for the isotropic solutions increased and  $B$ 's for both biphasic and fully anisotropic solutions were almost constant, with MW.

## INTRODUCTION

In our previous papers, we have presented the rheological properties of liquid crystalline hydroxypropyl cellulose (HPC) solutions at both low<sup>1,2</sup> and relatively high<sup>3-6</sup> shear rates. Our major findings were that (1) the concentration-temperature superposition for the shear viscosity could be applied, (2) the concentration dependence of the elastic parameters was similar to that of the viscosity, and (3) the elastic parameters at the capillary die entrance were related to other elastic parameters at the capillary die exit.

We also presented the static and dynamic mechanical properties of solid HPC films.<sup>7</sup> As a result of that research, it was ascertained that although HPC was a convenient model to investigate the anomalous liquid crystalline behav-

ior, it was not so important commercially. This is because HPC has a serious drawback of picking up the water from the atmosphere and being water-soluble. Therefore, we pay much attention to another liquid crystal-forming cellulose derivative which is not water-soluble, ethyl cellulose (EC).

EC has a limit in tensile properties compared with rigid-chain polymers, but seems to have a commercial availability of gas or liquid separation films.

TABLE I  
Characteristics of Unfractionated EC Used in This Study

	Viscometry <sup>a</sup>	GPC <sup>b</sup>				DS <sup>c</sup>		
	$\bar{M}_n$	$\bar{M}_n$	$\bar{M}_w$	$\bar{M}_z$	$\bar{M}_w/\bar{M}_n$			
EC-A	17,000	27,100	115,000	672,000	4.25	2.54	2.56	2.53
EC-B	23,000	37,800	123,000	247,000	3.26	2.67	2.67	2.61
EC-C	33,000	43,100	137,000	261,000	3.17	2.48	2.53	2.43
EC-D	40,000	58,600	187,000	—	3.12	2.49	2.56	2.43

<sup>a</sup> In benzene at 25°C,  $[\eta] = 2.92 \times 10^{-4} \bar{M}_n^{0.81}$ .

<sup>b</sup> In THF.

<sup>c</sup> By NMR.<sup>18</sup> Three determinations were made in each sample.

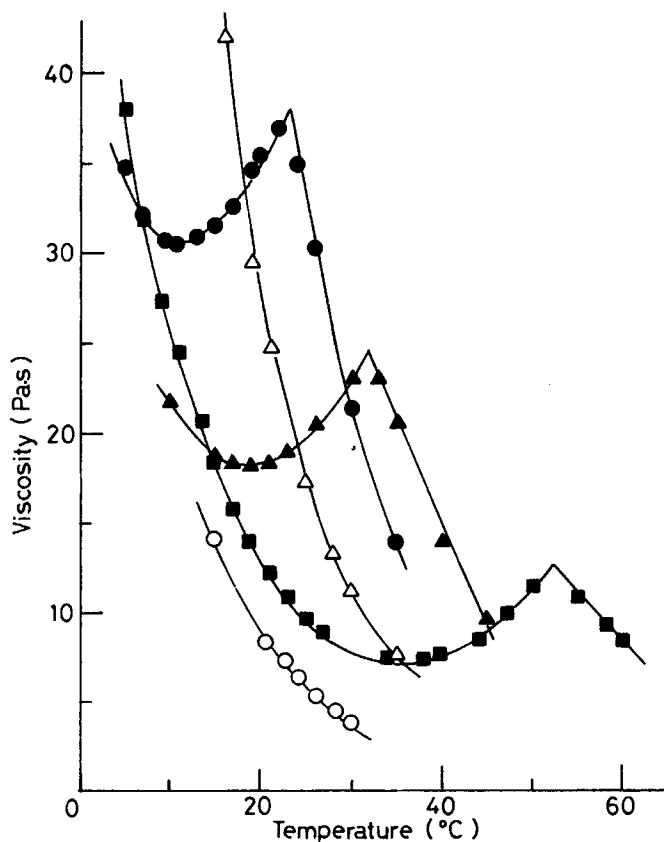


Fig. 1. Temperature dependence of shear viscosity for concentrated solutions of EC-A in *m*-cresol (wt %): (○) 25; (△) 30; (●) 33; (▲) 35; (■) 40.

Separation or permeation of gases through EC films and sorption of gases in EC films have been studied,<sup>8-11</sup> but none has discussed the applicability of the EC films to the gas or liquid separation from a standpoint of liquid crystalline films.

We presented the viscometric behavior and birefringence at rest of liquid crystalline EC solutions (cholesteric type<sup>12-14</sup>) and found the conditions for casting liquid crystalline EC films on the basis of the data for tensile creep *in vacuo*.<sup>15</sup> However, there were only few investigations on the rheology of liquid crystalline EC solutions.<sup>16</sup>

In this paper, we determine the rheological properties of liquid crystalline solutions of EC by means of two types of rheometer and discuss whether the rheological behavior observed for liquid crystalline HPC systems [(1)-(3) noted above] is valid for the EC systems or is fortuitous. We use four kinds of EC with different molecular weight and note the effects of molecular char-

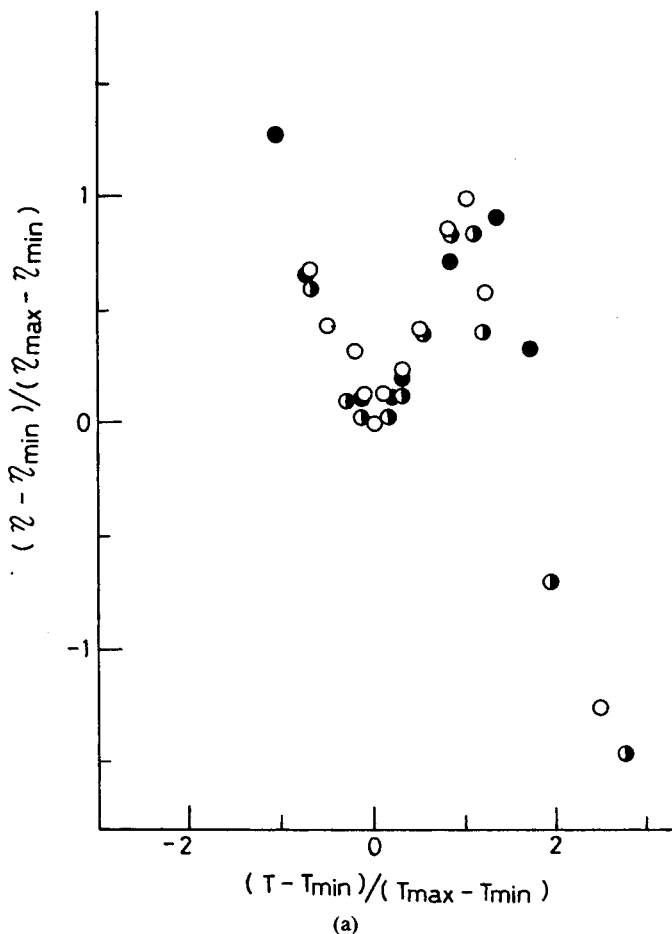


Fig. 2. Master curve for concentrated solutions (wt %) of (a) EC-A in *m*-cresol [(○) 33; (●) 35; (●) 40], (b) EC-C in *m*-cresol [(△) 33; (▲) 40], and (c) EC-D in *m*-cresol [(□) 33; (■) 40].

acteristics (molecular weight, distribution of molecular weight, and degree of substitution) on the rheology of liquid crystalline EC solutions.

## EXPERIMENTALS

### Samples

Four different EC samples used were of commercial reagent grade (Tokyo Kasei Kogyo Co. Ltd.). Those are abbreviated as EC-A, EC-B, EC-C, and EC-D in order of increasing molecular weight. Before use, EC powder was dried *in vacuo* at 60°C for about 24 h. Characterization data for the unfractionated samples referred to in this study are summarized in Table I. Reagent grade *m*-cresol was purchased from Wako Pure Chemical Ind., Ltd. and was purified by distillation at reduced pressure prior to use.

Intrinsic viscosities were measured in benzene with an Ubbelohde type viscometer in a water bath controlled within  $\pm 0.01^\circ\text{C}$  at 25°C. Both shear rate and kinetic energy corrections were negligible.

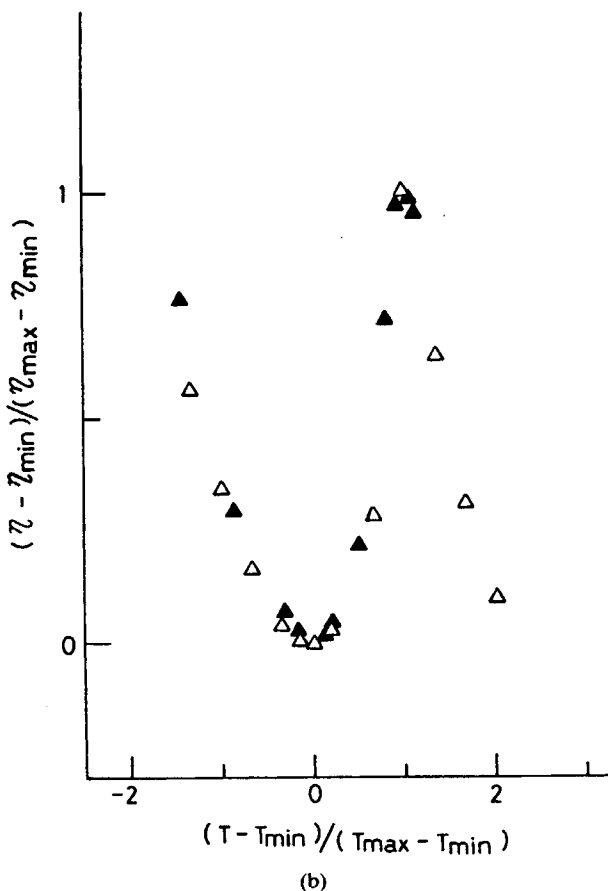


Fig. 2. (Continued from the previous page.)

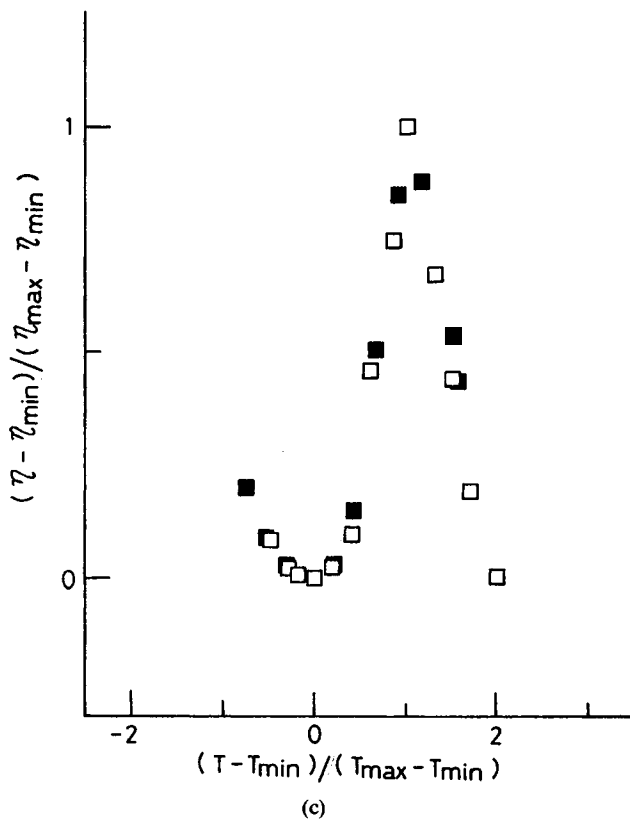


Fig. 2. (Continued from the previous page.)

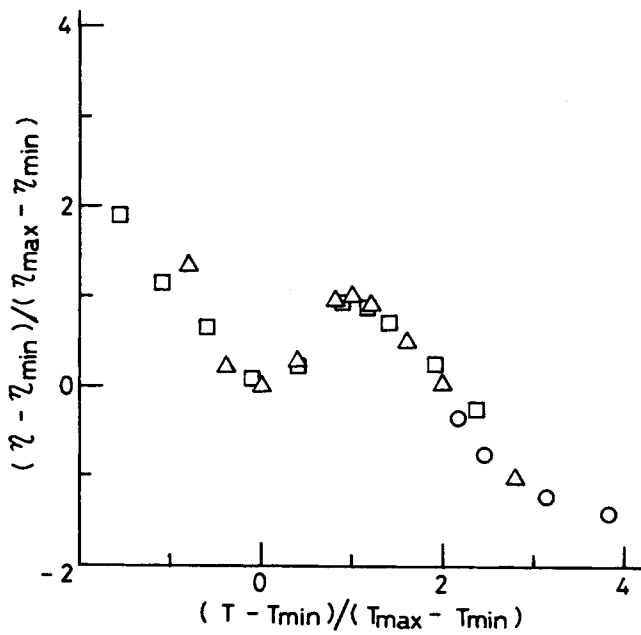


Fig. 3. Master curve for EC-A in benzyl alcohol. Concentration (wt %): (○) 45; (△) 50; (□) 55.

The number-average molecular weight  $\bar{M}_n$  of the samples was determined by the intrinsic viscosity  $[\eta]$  and the relation<sup>17</sup>

$$[\eta] = 2.92 \times 10^{-4} \bar{M}_n^{0.81}$$

The molecular weights and distribution of molecular weight were also measured in tetrahydrofuran solution by GPC. The degree of substitution (DS) of the samples were measured by the NMR technique, according to the procedure proposed by Clemett.<sup>18</sup>

### Preparation of Concentrated Solutions

A sample of 40–50 g of EC was weighted accurately into a glass-stoppered flask and a given amount of *m*-cresol was added. The mixture was stirred for

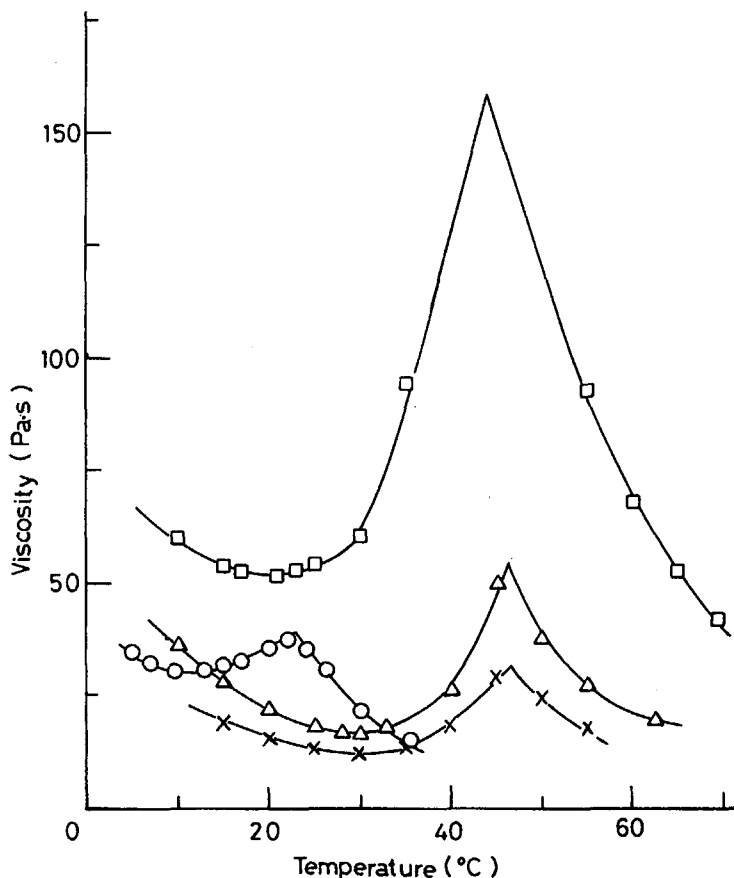


Fig. 4. Temperature dependence of shear viscosity for concentrated solutions of EC in *m*-cresol; concentration 33 wt %: (○) EC-A; (×) EC-B; (Δ) EC-C; (□) EC-D.

about a week and was then stored in the dark for about 3 months at room temperature. The concentration range of solutions was 25–40 wt %.

### Rheometry

A cone-plate type viscometer for a low shear rate ( $1 \text{ s}^{-1}$ ) and a capillary type rheometer for relatively high shear rates were used. The details of the measurements have been described in the Refs. 1–6. It must be emphasized that the solutions must be allowed to rest at least 45 min before starting measurements at a given temperature and shear rate.

The elastic parameters observed with the capillary rheometer were the Bagley coefficient factor ( $\nu$ ), the entrance pressure drop ( $\Delta P_{\text{ent}}$ ), and the die swell ( $B$ ).  $\nu$  and  $\Delta P_{\text{ent}}$  were parameters at the die entrance and  $B$  was that at the die exit. Capillary rheometry was made at  $25^\circ\text{C}$ .

## RESULTS AND DISCUSSION

### Shear Viscosity at a Low Shear Rate ( $1 \text{ s}^{-1}$ )

Figure 1 shows the temperature dependence of the shear viscosity for EC-A solutions in *m*-cresol. The viscosity exhibited a minimum ( $\eta_{\text{min}}$ ) and a maximum ( $\eta_{\text{max}}$ ) at critical temperatures designated  $T_{\text{min}}$  and  $T_{\text{max}}$ . This behavior was the same as that for HPC systems reported by us.<sup>1,2</sup> Consequently, we try

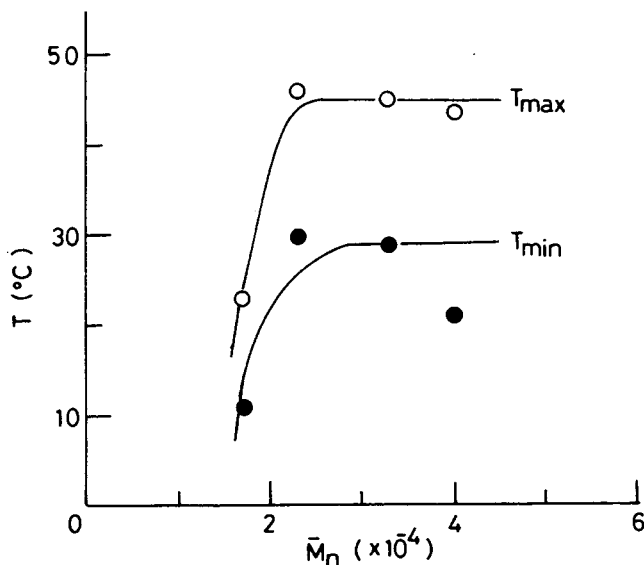


Fig. 5. Dependence of  $T_{\text{max}}$  and  $T_{\text{min}}$  on number-average molecular weight of EC. Concentration 33 wt %.

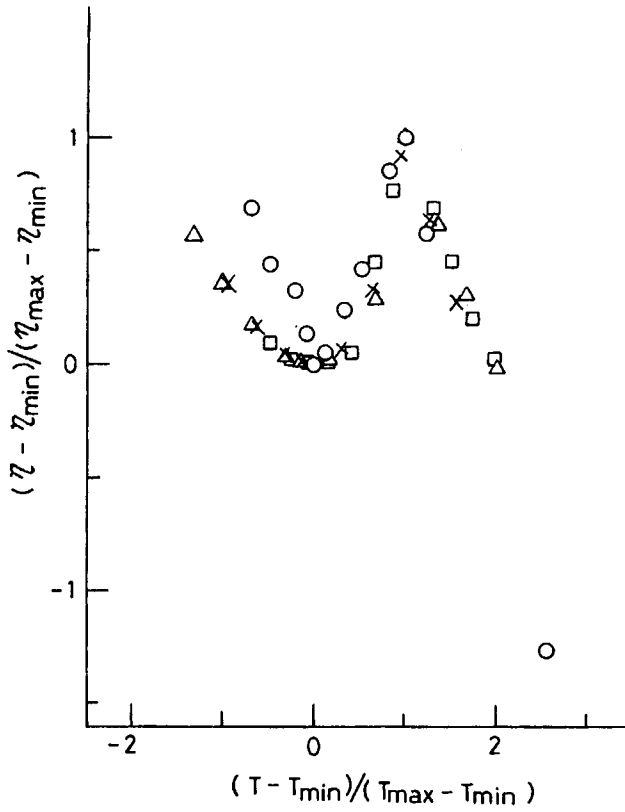


Fig. 6. Master curve for concentrated solutions of EC in *m*-cresol. Concentration 33 wt %. Notations as for Figure 4.

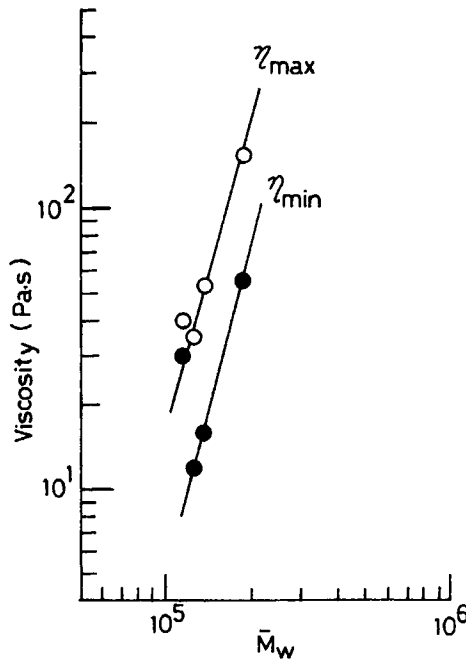


Fig. 7. Dependence of  $\eta_{\max}$  and  $\eta_{\min}$  on weight-average molecular weight of EC. Concentration 33 wt %.



to generate the viscometric behavior according to the same procedure as proposed by us<sup>1,2</sup>: normalizing both the ordinate and the abscissa. The concentration-temperature superposition for the results in Figure 1 is shown in Figure 2(a). Figures 2(b) and 2(c) show the same superposition for EC-C and EC-D, respectively. The superposition proposed by us could be clearly applied to EC/*m*-cresol systems. The results for another system, EC-A/benzyl alcohol, are shown in Figure 3. Thus, all lyotropic liquid crystalline systems of HPC and EC studied in our laboratory could be generalized by our procedure.<sup>1,2</sup> This strongly suggests that the concentration-temperature superposition for the shear viscosity at low shear rates is valid for lyotropic liquid crystals of cellulose derivatives. The simplicity of the viscometric behavior noted above indicates that the phase transformation dominates the viscometric behavior of the concentrated solutions of liquid crystal-forming cellulose derivatives: The shear viscosity for a given polymer/solvent system depends mainly on the volume of liquid crystalline phase.<sup>19,20</sup>

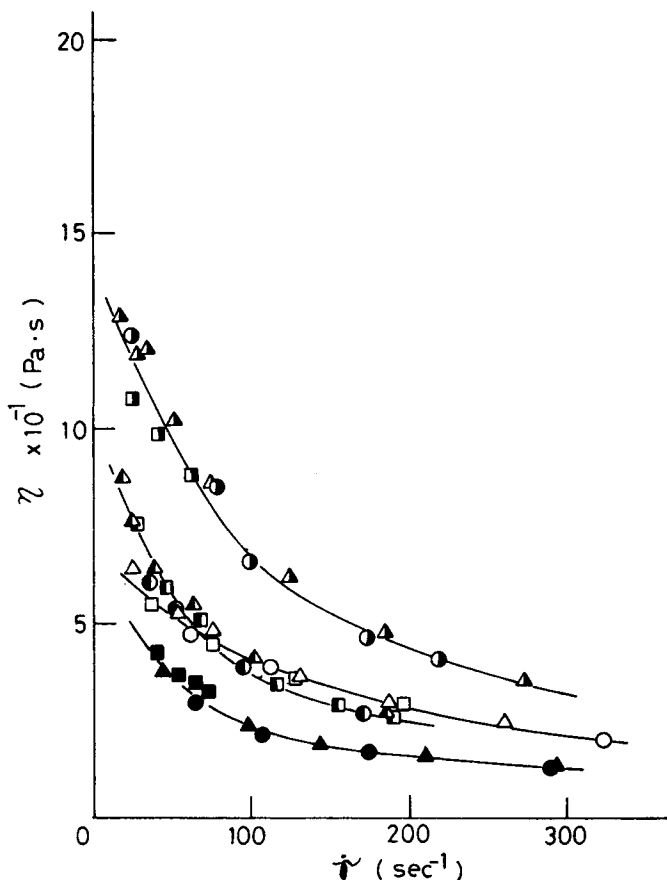


Fig. 8. Flow curves for concentrated solutions of EC-A in *m*-cresol (wt %) at 25°C: (○) 25; (◻) 30; (◻) 35; (●) 40.

In this study, four kinds of EC with different molecular weight (MW) were examined. The effect of MW on the viscometric behavior will be discussed. Figure 4 shows the temperature dependence of the shear viscosity for the 33 wt % solutions of each EC. The behavior of EC-A was quite different from the others:  $T_{\min}$  and  $T_{\max}$  for EC-A were smaller than those for the others. Gray et al.<sup>21</sup> and Ciferri et al.<sup>22</sup> have reported that when the critical concentration  $C_a$  or clearing temperature  $T_c$  is plotted against MW for cellulose derivatives,  $C_a$  or  $T_c$  is independent of MW above a critical MW.  $T_{\max}$  and  $T_{\min}$  for each EC sample are shown in Figure 5. Over the higher MW range than about  $2.5 \times 10^4$ ,  $T_{\max}$  (a critical temperature at which a phase transformation from biphasic to single isotropic regions occurs) and  $T_{\min}$  (a critical temperature at which a phase transformation from fully anisotropic to biphasic regions occurs) appeared to level off. This result was similar to those for the well-characterized fractionated samples reported by Gray et al.<sup>21</sup> and Ciferri et al.<sup>22</sup>; nevertheless, our samples were unfractionated.

The generalized plots for the results of the 33 wt % solutions in Figure 4 are shown in Figure 6. The curve for EC-A clearly deviated from those for the others. This deviation was pronounced over the entire range of temperature  $T < T_{\min}$ . The behavior for the 40 wt % solutions was similar to that shown in Figure 6. The viscometric behavior of lyotropic liquid crystals is affected by a

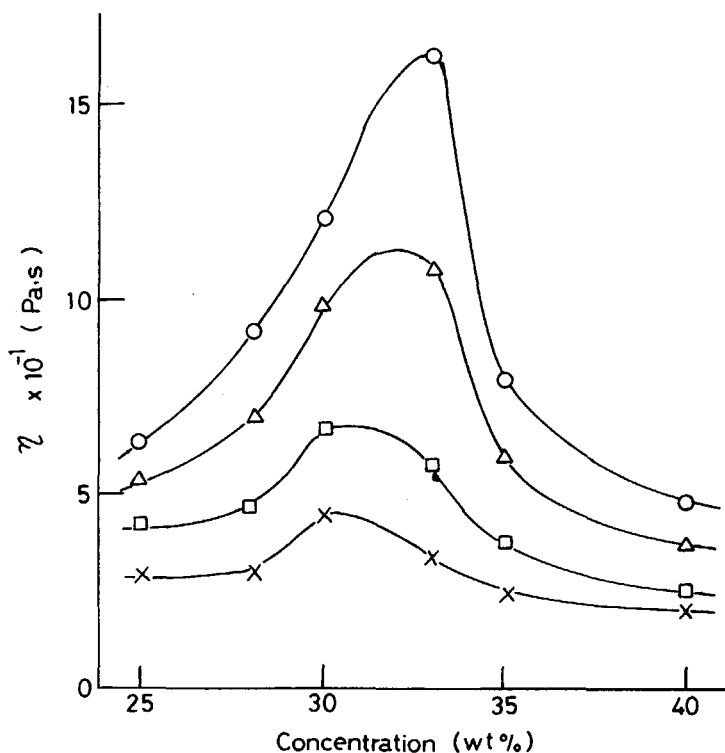


Fig. 9. Concentration dependence of shear viscosity  $\dot{\gamma}$  ( $s^{-1}$ ) for solutions of EC-A in *m*-cresol at 25°C: (○) 25; (Δ) 50; (□) 100; (×) 200.

number of molecular parameters, including MW, DMW, and DS. Obviously seen in Table I, DS for all ECs used in this study was the same, but DMW for EC-A was quite different from those for the others. Therefore, DMW may be a factor affected on the deviation of EC-A in Figure 6. However, we suppose, a size of the liquid crystalline domain is another factor affected on that deviation.<sup>2</sup> We will show the experimental evidence for our supposition noted above. The shape of the superposition curve for EC-A/*m*-cresol system was different from that for EC-A/benzyl alcohol system in the temperature range  $T < T_{\min}$ . Furthermore, for the solutions of a given HPC in different solvents the shape of the superposition curves was different from each other at fully anisotropic phase; nevertheless, DMW and MW of HPC are the same.<sup>1,2</sup> These indicate that a main factor is not DMW, but the size of liquid crystalline domain.

Our finding shown in Figure 6 suggests that the size of the liquid crystalline domain is strongly related to MW and is independent of MW above the critical MW. Wunder et al.<sup>23</sup> reported that the melt viscosity for thermotropic polyesters was sensitive to the domain size (smaller than 2  $\mu\text{m}$ ). The lyotropic liquid crystals of cellulose derivatives may also have a critical domain size at low shear rate region, but this is not clear now. Therefore, we need to

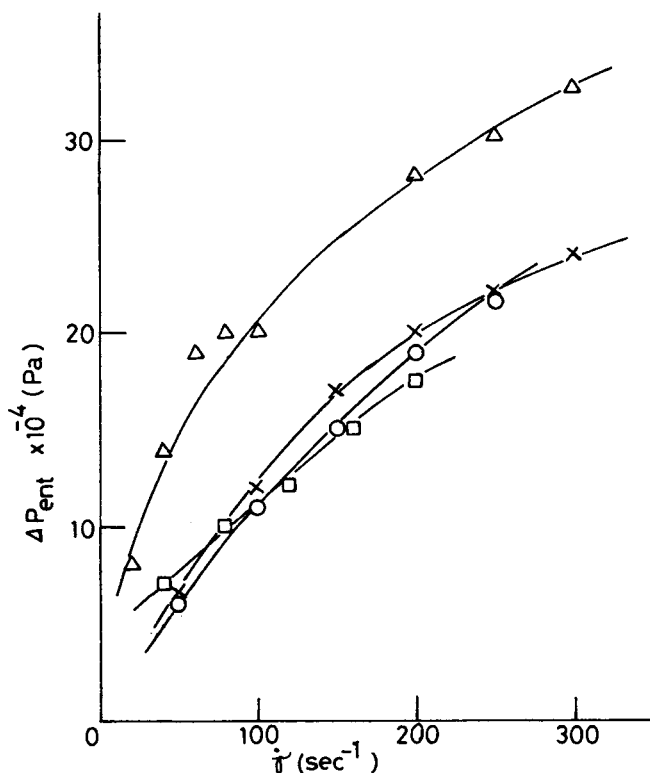


Fig. 10. Entrance pressure drop vs. shear rate for concentrated solutions (wt %) of EC-A in *m*-cresol at 25°C: (○) 25; (△) 30; (□) 35; (×) 40.

experimentally confirm the independency of the domain size above the critical MW by optical methods.

Figure 7 shows the dependence of  $\eta_{\max}$  and  $\eta_{\min}$  on MW for EC solutions. In this figure the weight-average molecular weight  $\bar{M}_w$  was used as the abscissa. The data except for EC-A formed a linear line and the slopes of the curves were about 4.14 for  $\eta_{\max}$  and about 6.5 for  $\eta_{\min}$ . Papkov et al.<sup>24</sup> showed in their study of the concentration dependence of the viscosity that the slope of the linear plot of  $\eta_{\max}$  vs.  $\bar{M}_w$  for poly(para-benzamide) solutions was 3.2; the value was very close to the universal value 3.4 for flexible polymers.<sup>25</sup> The value 4.14 in this study was greater than the value 3.2 observed by Papkov et al.<sup>24</sup> for the rigid polymer; nevertheless, our polymer is semirigid.<sup>21,22</sup> Furthermore, it is noteworthy that the  $\bar{M}_w$  dependence of  $\eta_{\min}$  is greater than that of  $\eta_{\max}$ . However, the range of  $\bar{M}_w$  covered in this study was very limited; therefore, the data over the wider range of  $\bar{M}_w$  were required.

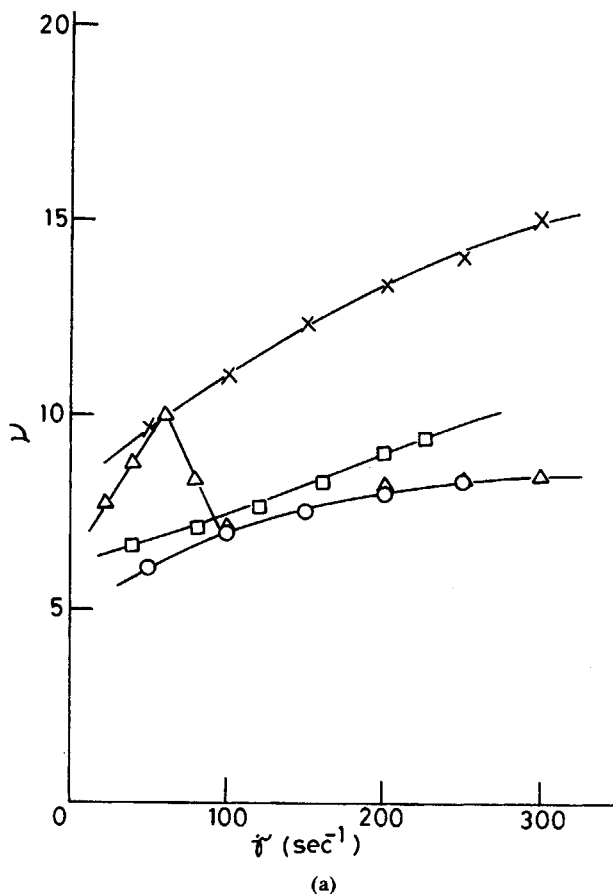


Fig. 11. Bagley correction factor vs. shear rate for concentrated solutions (wt %) of (a) EC-A in *m*-cresol [(○) 25; (Δ) 30; (□) 35; (×) 40], (b) EC-C in *m*-cresol [(○) 25; (Δ) 33; (×) 40], and (c) EC-D in *m*-cresol at 25°C [(○) 25; (Δ) 33; (×) 40].

### Shear Viscosity at Relatively High Shear Rate

As our previous papers showed,<sup>5,6</sup> the so-called Bagley end correction was applicable to our systems in this study: the plot of the pressure drop ( $\Delta P$ ) against the ratio of the die length ( $L$ ) to the die diameter ( $D$ ),  $L/D$ , was linear. In this Bagley procedure, the following is worthy to note: In a strict sense, the linear relation for the biphasic solutions of EC-A seemed to be not so good as that for the single phase solutions (isotropic and anisotropic) and as that for the other EC solutions. This will be due to the wider DMW as shown in Table I. However, this problem is not so serious and the trends to be discussed later are quite definite.

Figure 8 shows the shear rate dependence of the true shear viscosity of EC-A for each concentration. A marked shear thinning at low shear rate region was observed, and this tendency became distinct as the concentration

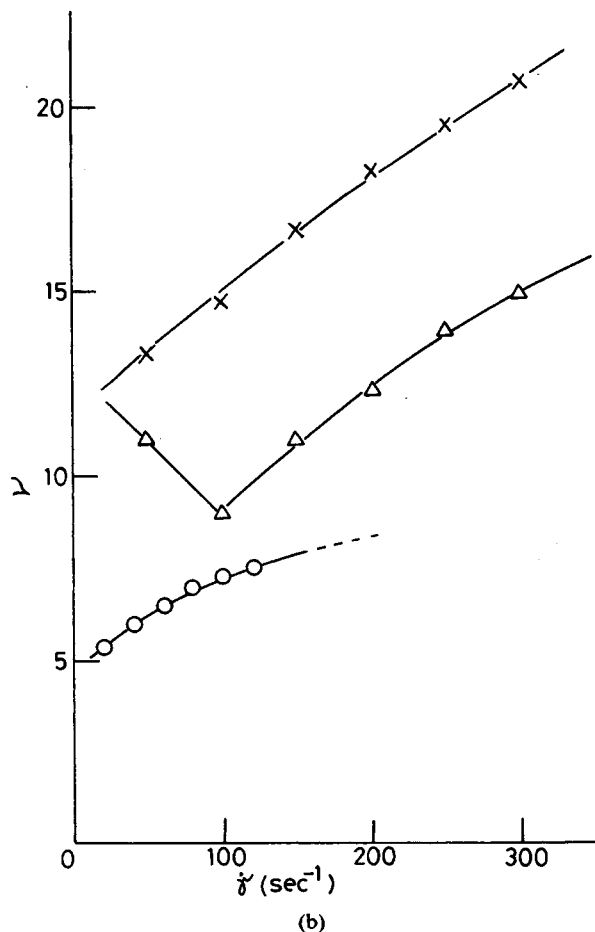
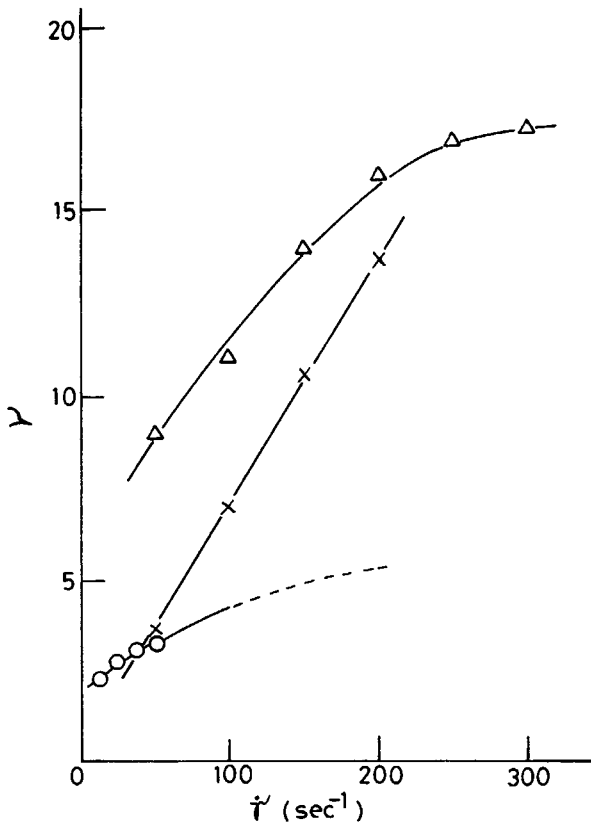


Fig. 11. (Continued from the previous page.)

increased. This behavior is the same as that for HPC systems.<sup>5,6</sup> In this Figure 8, data for the 28 and 33 wt % solutions were not shown because of avoiding overlap of the each curve. The viscometric behavior for the other EC samples was similar to that shown in Figure 8. This shear thinning of the viscosity at very low shear rates is typical behavior for polymeric liquid crystals of both lyotropic and thermotropic.<sup>26</sup> Another feature in Figure 8 was that the plateau region (region II proposed by Onogi and Asada<sup>27</sup>) was missing.

Figure 9 shows the concentration dependence of the true shear viscosity of EC-A at given shear rates. This behavior is typical of the viscosity for polymeric liquid crystals<sup>26</sup>: the viscosity shows the maximum and minimum which become less pronounced and shift to lower concentration as shear rate increases. When we recognize the maximum as a measure of the onset of liquid crystalline phase, the maximum shift to lower concentration suggests the shear-induced liquid crystallization which was shown for another semirigid polymer.<sup>28</sup> Furthermore, based on the behavior of the decreasing maximum value with shear rate, we can easily estimate that at a given shear rate the maximum and minimum will disappear and above the critical shear rate the



(c)

Fig. 11. (Continued from the previous page.)

viscosity will increase monotonically with polymer concentration. The disappearance of the viscosity maximum and minimum has reported for poly(benzyl glutamate) solutions in *m*-cresol by Kiss and Porter.<sup>29</sup> The monotonical increase in the viscosity with polymer concentration for liquid crystalline solutions is similar to the flow behavior for the extended flexible chain polymers.<sup>30</sup> There should be difference between the behavior above a critical shear rate for the liquid crystals and for the extended flexible polymer: stress relaxation after shear cessation.<sup>31</sup>

At any event, the shear rate and concentration dependence of the shear viscosity at relatively high shear rates for EC solutions was quite similar to that for HPC solutions.<sup>5,6</sup>

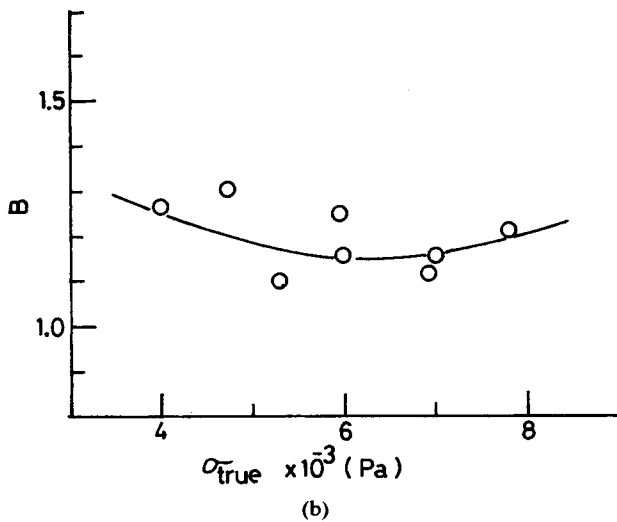
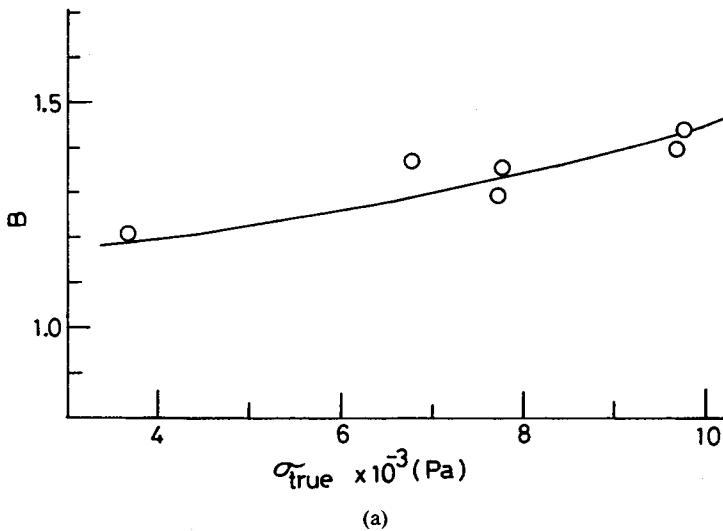


Fig. 12. Die swell vs. shear stress for concentrated solutions of EC-A in *m*-cresol at 25°C. Concentration (wt %): (a) 30; (b) 33; (c) 35; (d) 40.

### Elastic Parameters at Relatively High Shear Rates

Figure 10 shows the shear rate dependence of the entrance pressure drop ( $\Delta P_{\text{ent}}$ ) for given concentrations of EC-A solution.  $\Delta P_{\text{ent}}$  increased with increasing shear rate for isotropic, biphasic, and fully anisotropic phases.

Figure 11(a) shows the shear rate dependence of the Bagley correction factor ( $\nu$ ) for the same system as shown in Figure 10. The behavior of  $\nu$  was little different from that of  $\Delta P_{\text{ent}}$ :  $\nu$  for the 30 wt % solution exhibited a maximum and a minimum. The  $\nu$  behavior for the other EC systems was shown in Figs. 11(b) and 11(c); for EC-C system the 33 wt % solution showed a minimum, and for EC-D system no maximum and minimum was exhibited. The dependence of  $\nu$  on the shear rate seemed to be dependent on whether

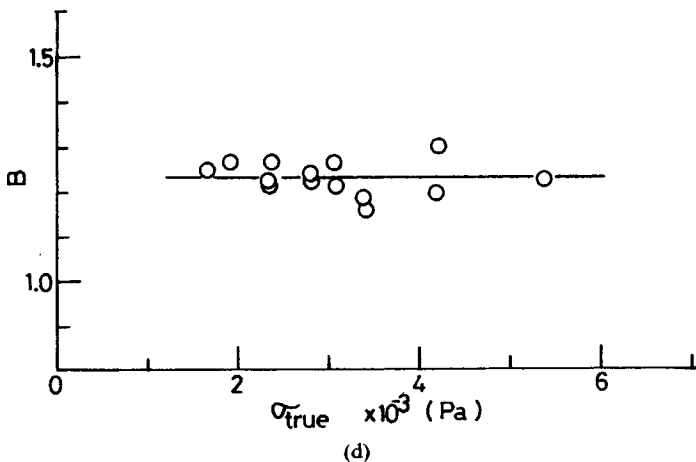
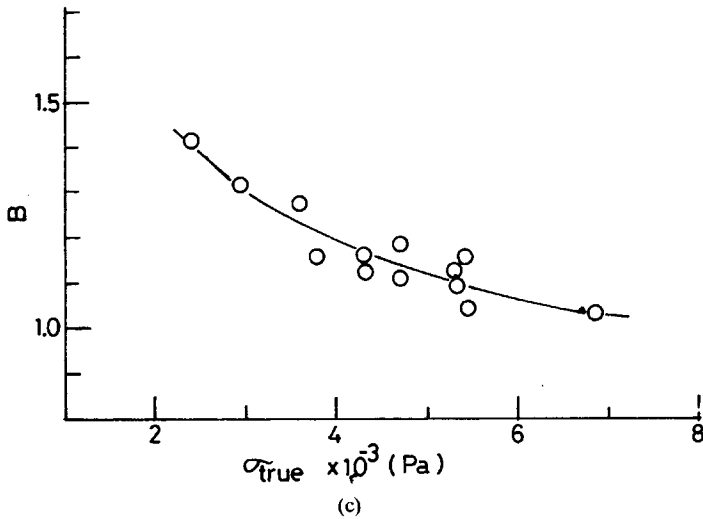


Fig. 12. (Continued from the previous page.)



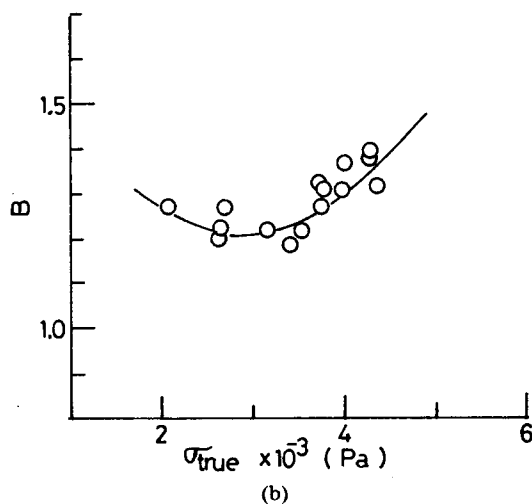
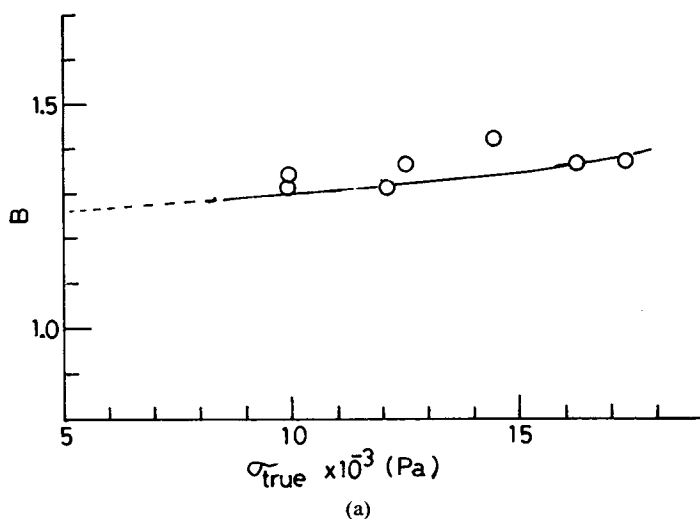


Fig. 13. Die swell vs. shear stress for concentrated solutions of EC-D in *m*-cresol at 25°C. Concentration (wt %): (a) 25; (b) 33; (c) 40.

the solution concentration is in single phase region or biphasic one:  $\nu$  behaved monotonically for single phase solutions but did not for biphasic solutions. Generally,  $\nu$  increases with shear rate for isotropic melts.<sup>32-34</sup> The behavior of  $\nu$  for biphasic solutions was quite similar to that for poly(vinyl chloride) copolymer<sup>35</sup> and to that for maltose slops.<sup>36</sup> It is well-known that molten poly(vinyl chloride) is not perfectly isotropic but includes crystallites.<sup>37</sup> Maltose slops may form a liquid crystal in suitable conditions.

Figures 12 and 13 show the dependence of the die swell ( $B$ ) on the true shear stress.  $B$  could not be determined at relatively low shear stresses for the isotropic solutions of EC-A, because of pronounced gravitational sagging.

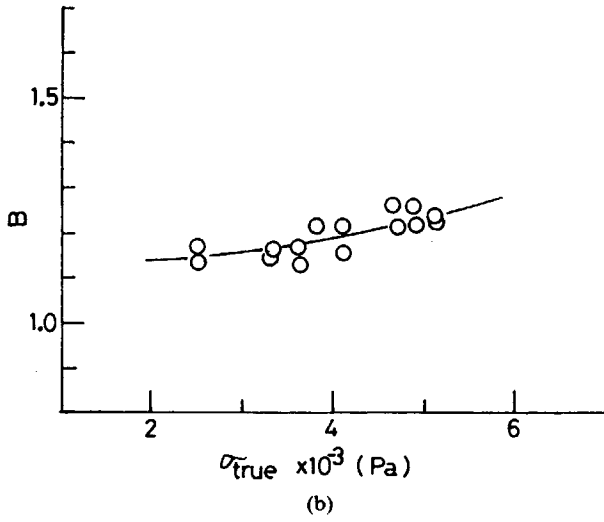
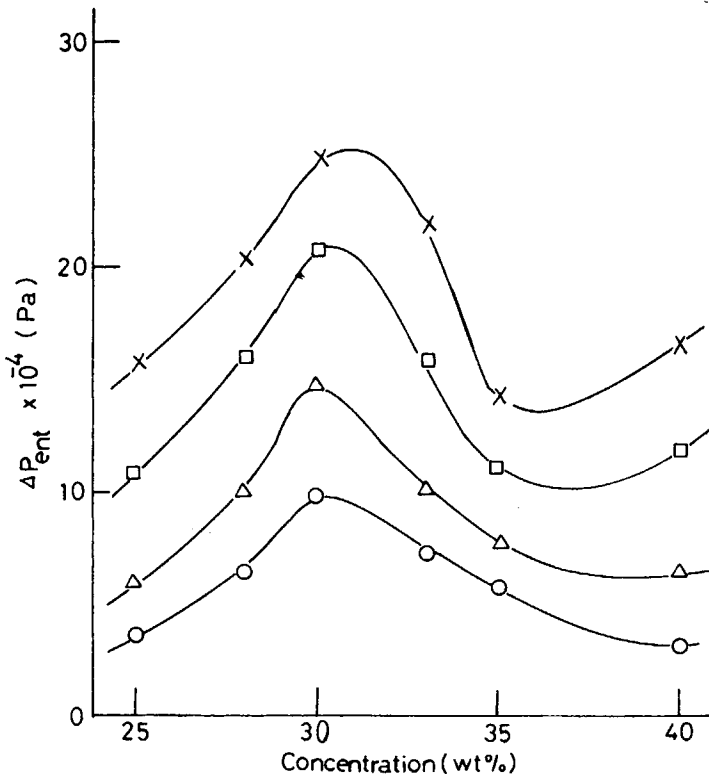


Fig. 13. (Continued from the previous page.)

Fig. 14. Concentration dependence of entrance pressure drop for concentrated solutions of EC-A in *m*-cresol at 25°C.  $\dot{\gamma}$  ( $\text{s}^{-1}$ ): (○) 25; (Δ) 50; (□) 100; (×) 150.

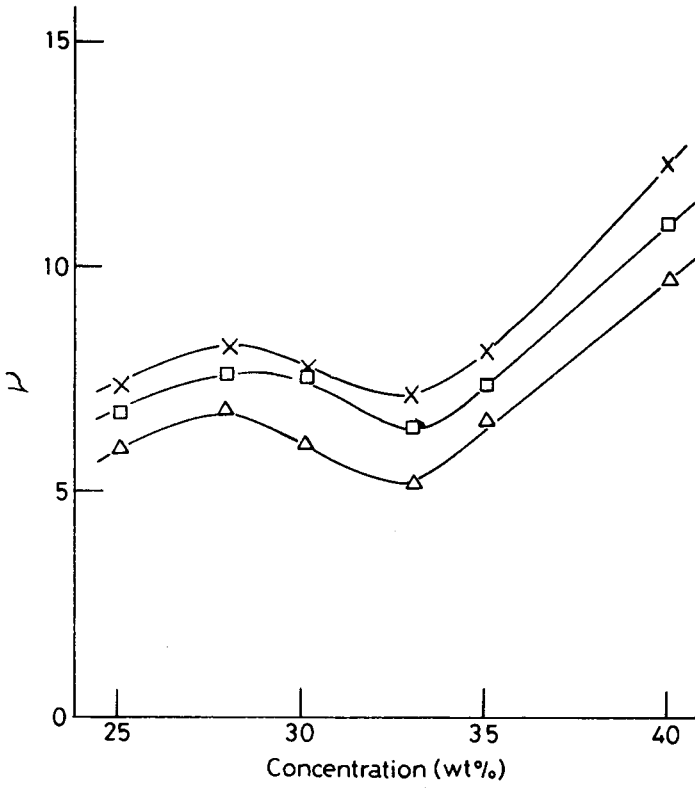


Fig. 15. Concentration dependence of Bagley correction factor for concentrated solutions of EC-A in *m*-cresol at 25°C.  $\dot{\gamma}$  ( $\text{s}^{-1}$ ): ( $\Delta$ ) 50; ( $\square$ ) 100; ( $\times$ ) 150.

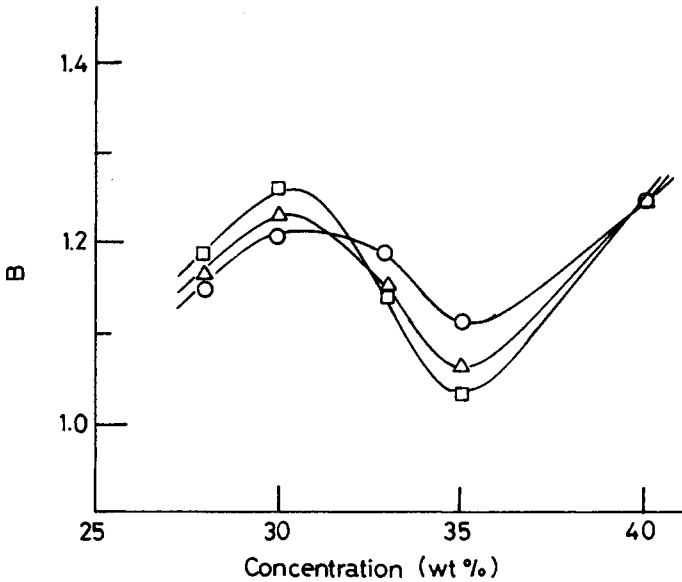


Fig. 16. Concentration dependence of die swell for concentrated solutions of EC-A in *m*-cresol at 25°C.  $\sigma_{\text{true}} \times 10^{-3}$  (Pa): ( $\circ$ ) 5.0; ( $\Delta$ ) 6.0; ( $\square$ ) 7.0.

Figures 12(a), 12(b), 12(c), and 12(d) show the behavior of  $B$  for the 30, 33, 35, and 40 wt % solutions of EC-A, respectively.  $B$  increased with shear stress for the 30 wt %, showed a minimum for the 33 wt %, decreased with for the 35 wt %, and was almost constant for the 40 wt % solution in our shear range. Figures 13(a), 13(b), and 13(c) show the behavior of  $B$  for the 25, 33, and 40 wt % solutions of EC-D. The behavior of  $B$  for the EC-D solutions was similar to that for the EC-A solutions, except the 40 wt % solution increased with shear.

Compared with the results of HPC solutions reported previously by us,<sup>5,6</sup> the behavior of  $\nu$  or  $B$  for EC solutions was not the same as that for HPC solutions with respect to shear rate or stress; first, the maximum or minimum of  $\nu$  for a given concentration of EC solutions was never observed for HPC solutions in our limited conditions, secondly, the shear stress dependence of  $B$  for EC solutions was not so great as that for HPC solutions and  $B$  for given

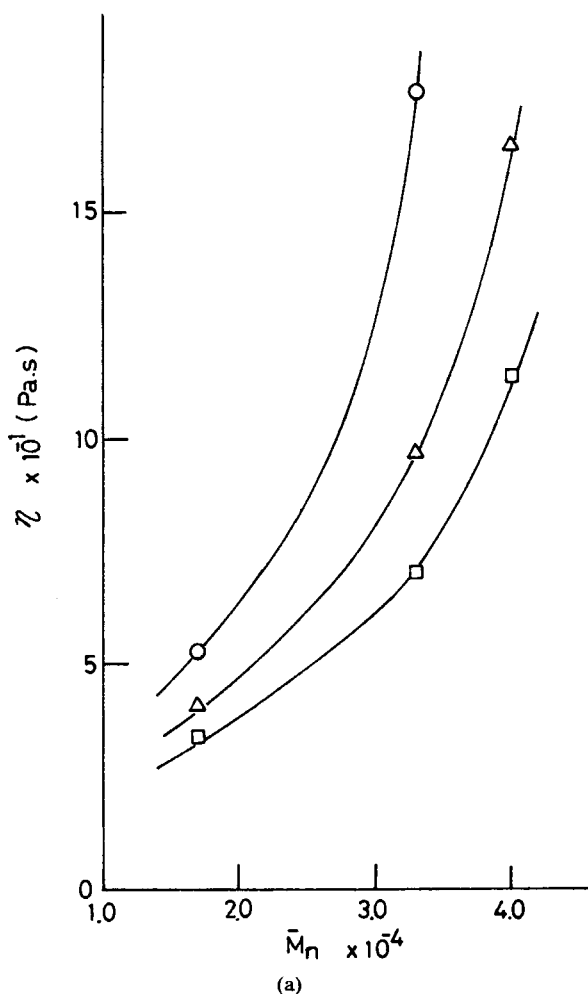


Fig. 17. Dependence of shear viscosity on number-average molecular weight of EC at 25°C. Concentration (wt %): (a) 25; (b) 33; (c) 40.  $\dot{\gamma}$  ( $s^{-1}$ ): (○) 50; (△) 100; (□) 150.

concentrations (biphasic region) exhibited a minimum with respect to shear stress in contrast with the HPC solutions which showed a maximum for the biphasic region. However, the behavior of  $\nu$  or  $B$  for EC solutions was essentially similar to that of HPC solutions with respect to shear rate or shear stress.

Figure 14 shows the concentration dependence of  $\Delta P_{\text{ent}}$  for EC-A at given shear rates.  $\Delta P_{\text{ent}}$  showed a maximum and a minimum. Figures 15 and 16 show  $\nu$  and  $B$  behavior with respect to concentration for EC-A.  $\nu$  and  $B$  also exhibited a maximum and a minimum. The concentration dependence of three elastic parameters noted above was very similar to that of the shear viscosity shown in Figure 9 and to those of the three elastic parameters and of the shear viscosity for HPC solutions.<sup>5,6</sup> However, it should be noted that the concentrations at the maximum or minimum were not always identical to each other parameter: the maximum and minimum of the viscosity corresponded to those of both  $B$  and  $\Delta P_{\text{ent}}$ , but did not to those of  $\nu$ . Kiss and Porter<sup>29</sup> and Baird<sup>38</sup> have reported that the concentration dependence of elastic parameters such as first normal stress difference  $N_1$  and the primary normal stress coefficient  $N_1/\dot{\gamma}^2$  was similar to that of viscosity, except for  $N_1/2\sigma$ , and that the phase transformation from isotropic to anisotropic phase affected the elastic parameters in a manner similar to viscosity. Therefore, the

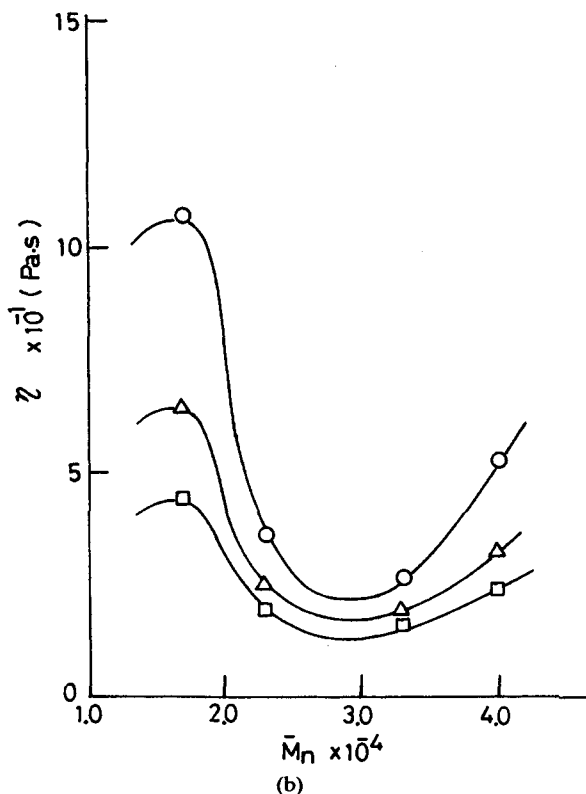


Fig. 17. (Continued from the previous page.)

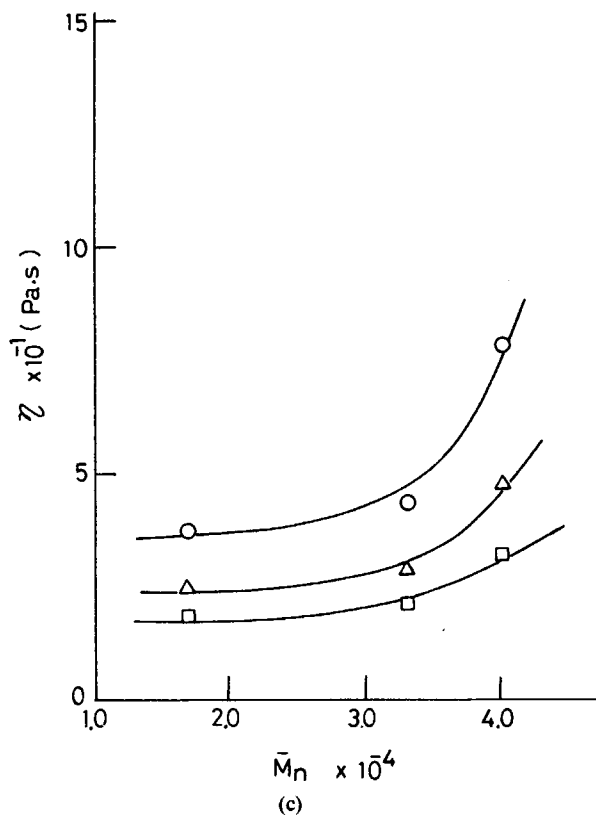
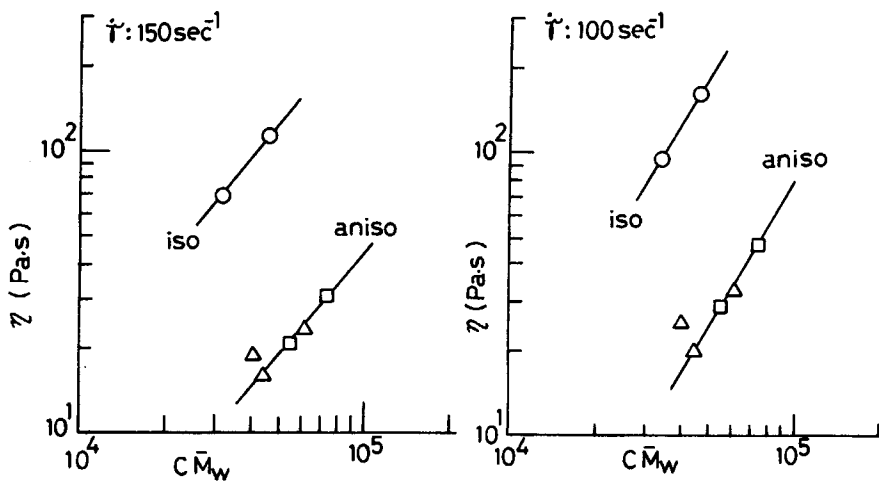


Fig. 17. (Continued from the previous page.)

Fig. 18. Dependence of shear viscosity on  $C\bar{M}_w$  at 25°C.

discrepancy of the maximum or minimum points between  $\nu$  and viscosity in our studies was unusual. Some investigators<sup>32,39-41</sup> have reported that  $\nu$  and  $\Delta P_{ent}$  for isotropic solutions and melts are not fully elastic parameters, but both elasticity and viscosity contribute to those parameters. However, the discrepancy noted above could not be explained in terms of the different magnitude of the elasticity contribution to  $\nu$ , because that discrepancy could not be observed between viscosity and  $\Delta P_{ent}$ , which was obtained by the same

TABLE II  
Values of Power Index  $n$  from  $\eta \propto (C\bar{M}_w)^n$  at 25°C

Shear rate ( $s^{-1}$ )	Isotropic	Fully anisotropic
1	3.64	2.42
50	—	2.19
100	1.66	1.74
150	1.53	1.24

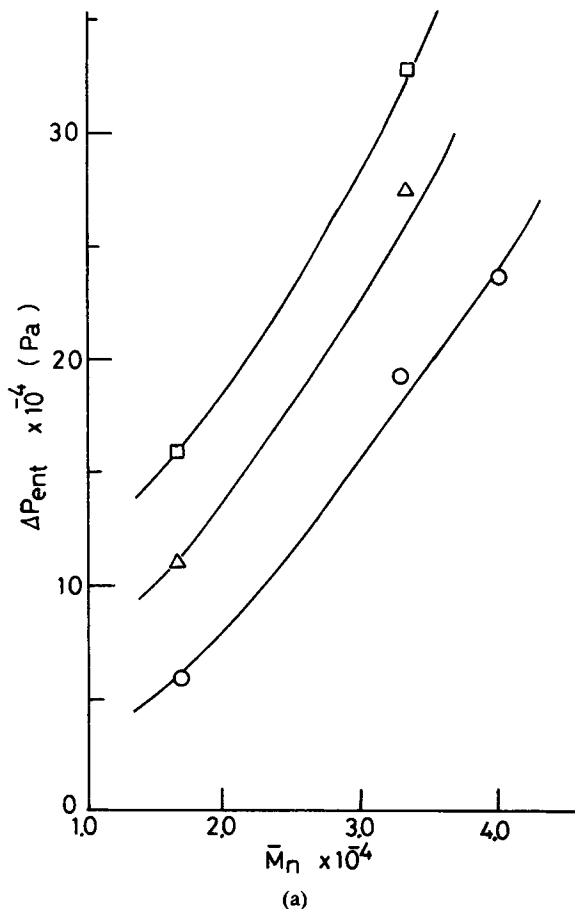


Fig. 19. Dependence of entrance pressure drop on number-average molecular weight of EC at 25°C. Concentration (wt %): (a) 25; (b) 33; (c) 40.  $\dot{\gamma}$  ( $s^{-1}$ ): (○) 50; (△) 100; (□) 150.

procedure as  $\nu$  was. This discrepancy in our studies need to be investigated further.

### Effect of MW on the Viscoelasticity at Relatively High Shear Rates

#### Shear Viscosity

Figures 17(a), 17(b), and 17(c) show the dependence of the shear viscosity on MW at given shear rates for the 25, 33, and 40 wt % solutions, respectively. The viscosity for the 25 or 40 wt % solution increased monotonically with MW, whereas the viscosity for the 33 wt % solution exhibited a minimum. This is because the 25 wt % solutions are isotropic, the 40 wt % solutions are fully anisotropic, and the 33 wt % solutions of EC-A and EC-B are biphasic and the others are fully anisotropic in our experimental range. This behavior was quite similar to that for poly(para-benzamide).<sup>24</sup>

It is well known that the zero-shear viscosity ( $\eta_0$ ) is proportional to  $(\overline{CM}_w)^3$  for flexible polymers and to  $(\overline{CM}_w)^{6-8}$  for rigid polymers.<sup>26</sup>  $\eta_0$  for liquid

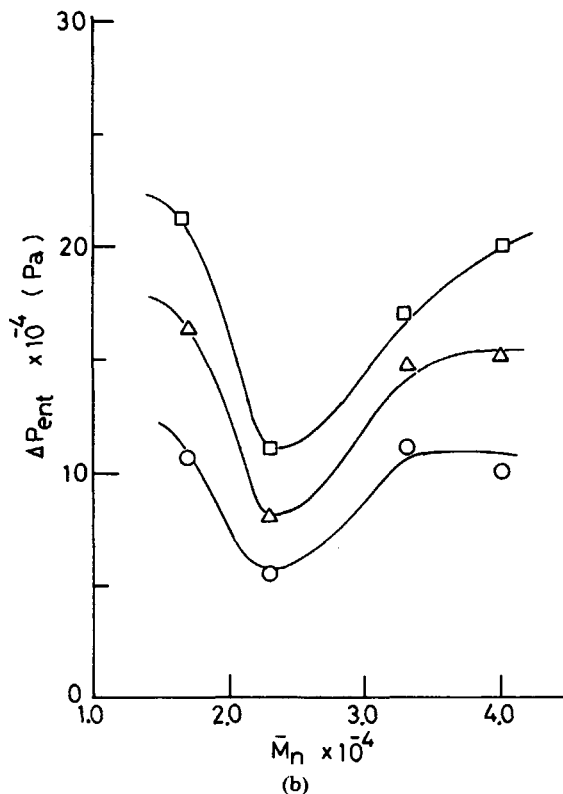
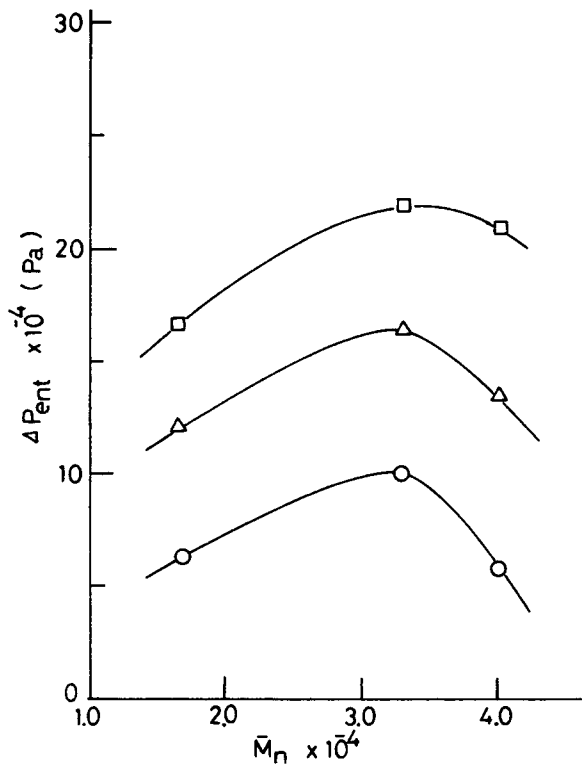


Fig. 19. (Continued from the previous page.)



crystalline solutions cannot be determined because those solutions have a pronounced yield stress. As apparently seen from Figure 8, the region II viscosity named by Onogi and Asada<sup>27</sup> could not also be measured for our liquid crystalline systems. Therefore, we cannot investigate the effect of MW on the viscometric behavior for the liquid crystalline phase according to the formulae noted above. In this study, however, we use the shear viscosity at given shears (not a specific parameter) as an alternative to  $\eta_0$  and try to qualitatively compare the dependence of viscosity on MW for fully anisotropic solutions with that for the isotropic ones.

Now, the product  $C\bar{M}_w$  is used as the abscissa and the data in Figure 17 are plotted in a log-log manner in Figures 18 for each shear rate. The data for EC-A were omitted from Figures 18 because we eliminate the effect of DMW on the viscometric behavior. It appeared that the viscosity at a given shear rate for a single phase (isotropic and anisotropic) linearly increased with  $C\bar{M}_w$ . The slopes of the linear curves for the isotropic region and the fully anisotropic region are shown in Table II. It was noteworthy that the MW dependence of the viscosity was dependent on shear rate: The larger MW sensitivity of the viscosity, the lower shear rate. Furthermore, it seemed that



(c)

Fig. 19. (Continued from the previous page.)

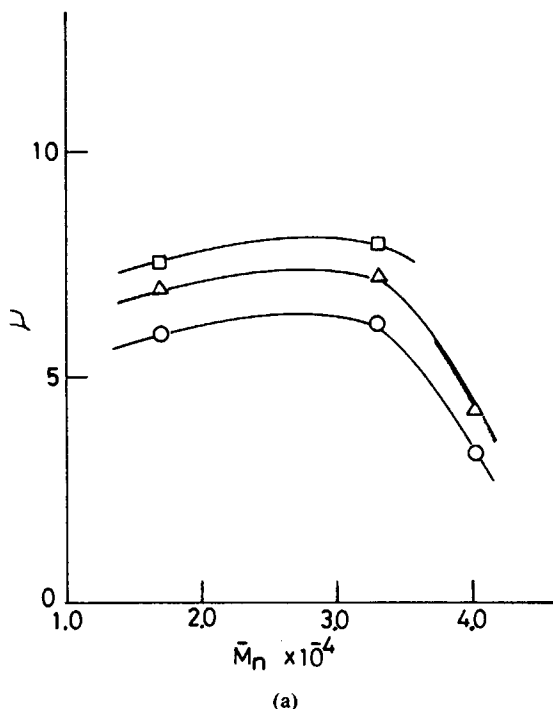


Fig. 20. Dependence of Bagley correction factor on number-average molecular weight of EC at 25°C. Concentration (wt %): (a) 25; (b) 33; (c) 40.  $\dot{\gamma}$  ( $\text{s}^{-1}$ ): (○) 50; (Δ) 100; (□) 150.

the dependence of the viscosity on MW for the isotropic solutions was stronger than that for the fully anisotropic solutions. This behavior was the same as that reported by Blumstein et al.<sup>42</sup> for semirigid polymers (nematic type). However, the data for the isotropic region (only two points) were very few, and we cannot conclude definitely the dependence noted above. Supplemental experiments are planning on that point.

#### *Elastic Parameters*

Figures 19(a), 19(b), and 19(c) show the dependence of  $\Delta P_{\text{ent}}$  on the number-average molecular weight  $\bar{M}_n$  for the 25, 33, and 40 wt % solutions, respectively.  $\Delta P_{\text{ent}}$  increased with  $\bar{M}_n$  for the isotropic 25 wt % solutions, exhibited a minimum for the 33 wt % solutions, and exhibited a maximum for the 40 wt % solutions (fully anisotropic).

Figures 20(a), 20(b), and 20(c) show the dependence of  $\nu$  on  $\bar{M}_n$  for the 25, 33, and 40 wt % solutions.  $\nu$ 's of the 25 and 40 wt % solutions showed a maximum and  $\nu$  of the 33 wt % solutions monotonically increased with  $\bar{M}_n$ . When the  $\bar{M}_n$  dependence of  $\Delta P_{\text{ent}}$  is compared with that of  $\nu$  for each concentration, there is a great difference between them except for the 40 wt % solution. In comparison with the viscosity shown in Figure 17, the behavior of

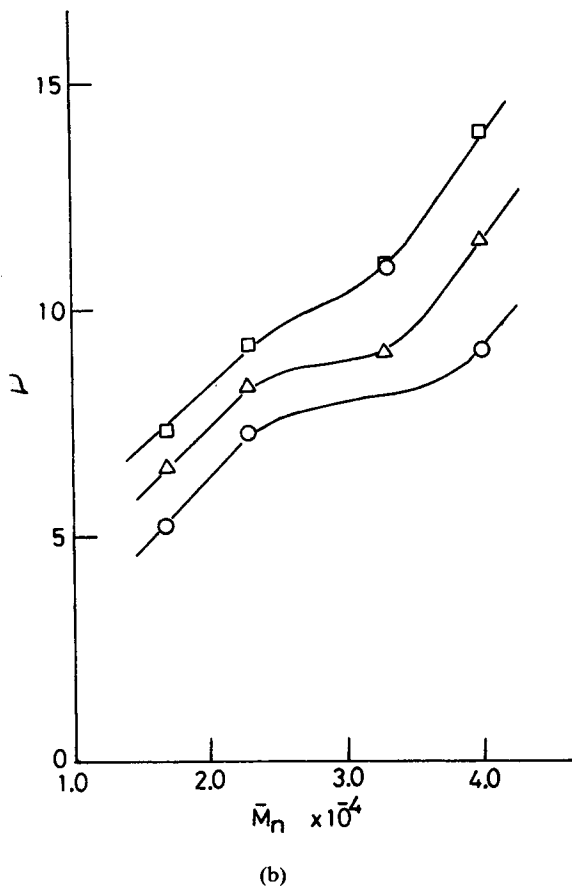
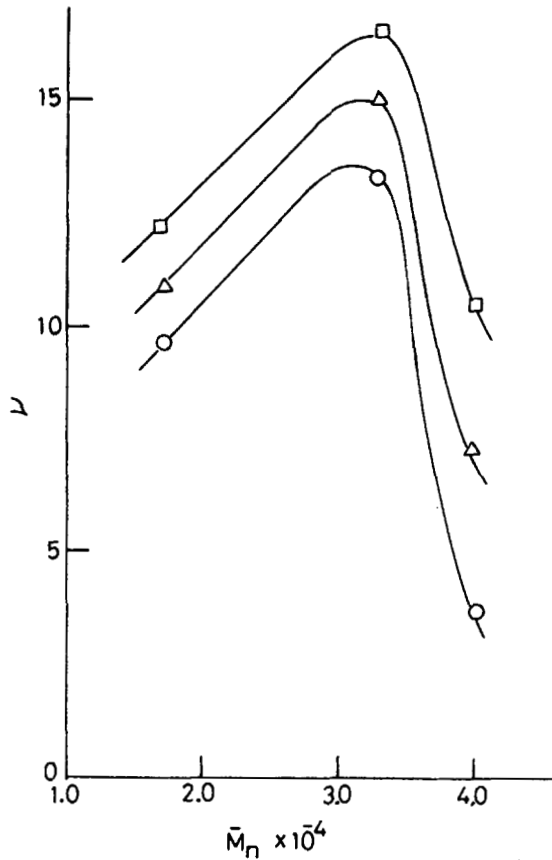


Fig. 20. (Continued from the previous page.)

$\Delta P_{\text{ent}}$  was very similar to that of the viscosity for the 25 and 33 wt % solutions but was not for the 40 wt % solution. Consequently, there is no similarity between two elastic parameters ( $\nu$  and  $\Delta P_{\text{ent}}$ ) and viscosity with respect to  $\bar{M}_n$ . It is not clear now why the  $\bar{M}_n$  dependence of the viscosity was not fully consistent with that of the elastic parameters.

The most obvious elastic parameter during capillary extrusion is  $B$ . Figures 21(a), 21(b), and 21(c) show the dependence of  $B$  on  $\bar{M}_n$  for the 25, 33, and 40 wt % solutions.  $B$  for the 25 wt % solutions tended to increase with  $\bar{M}_n$ , and  $B$  for the 33 and 40 wt % solutions was almost independent of  $\bar{M}_n$ . Generally,  $B$  for the isotropic polymer melts increased with increasing MW and DMW.<sup>43-45</sup> Therefore,  $B$  for the biphasic or fully anisotropic solution of EC system seemed to be different from that for the isotropic melts. Unfortunately, we cannot express clearly the  $\bar{M}_n$  dependence of  $B$  for the anisotropic solutions because of the narrow range of MW covered. However, the limited data suggest that the dependence of  $B$  on MW is not so great as that of the viscosity on MW for EC solutions.



(c)

Fig. 20. (Continued from the previous page.)

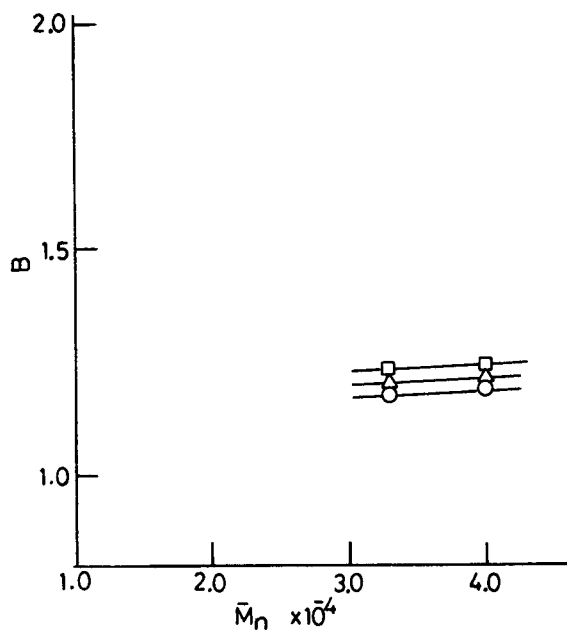
## CONCLUSIONS

From the results of this study for four EC samples with different MW, the following can be concluded:

1. Shear viscosity at  $\dot{\gamma} = 1 \text{ s}^{-1}$  exhibited a minimum ( $\eta_{\min}$ ) and a maximum ( $\eta_{\max}$ ) with respect to temperature, and the concentration-temperature superposition for the shear viscosity could be applied. This behavior was the same as that for HPC solutions reported by us.<sup>1,2</sup> The superposition curves for each MW sample of EC overlapped beyond a given MW, and this behavior seemed to be attributed to the size of liquid crystalline domain. The MW dependence of  $\eta_{\min}$  was greater than that of  $\eta_{\max}$ .

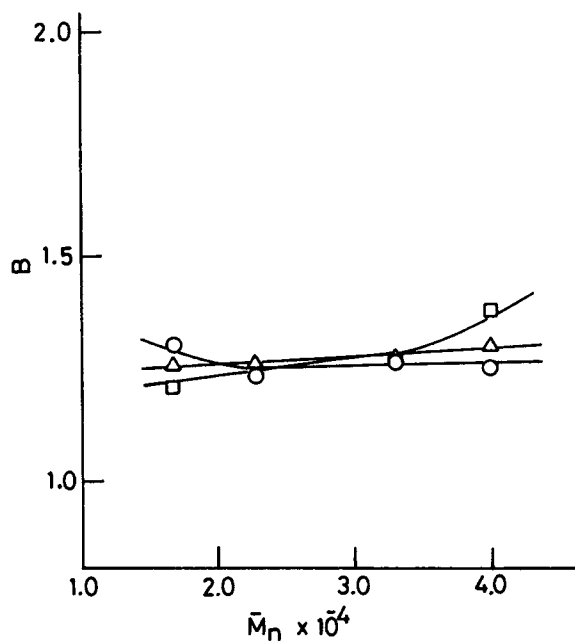
2. The behavior of the shear viscosity at relatively high shear rates was typical of the lyotropic liquid crystals with respect to shear rate or polymer concentration,<sup>26</sup> and was the same as that reported previously by us.<sup>5,6</sup>

3. The shear rate or stress dependence of the elastic parameters at relatively high shear rates was greatly dependent on whether the polymer solution was in the single or biphasic region; the isotropic or fully anisotropic solution behaved relatively monotonically, but the biphasic solution did not.



(a)

Fig. 21. Dependence of die swell on number-average molecular weight of EC at 25°C. Concentration (wt %): (a) 25; (b) 33; (c) 40.  $\sigma_{\text{true}} \times 10^{-3}$  (Pa): (a) (○) 5.0; (△) 6.0; (□) 7.0; (b, c) (○) 3.0; (△) 4.0; (□) 5.0.



(b)

Fig. 21. (Continued from the previous page.)

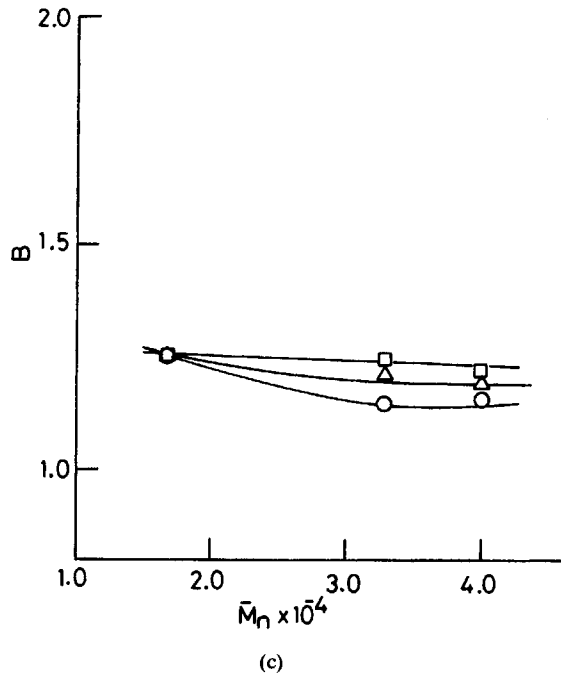


Fig. 21. (Continued from the previous page.)

With respect to concentration the elastic parameters showed a maximum and a minimum, and the maximum or minimum point for each parameter was not always identical to each other. The behavior of the elastic parameters for EC solutions was essentially similar to that for HPC solutions,<sup>5,6</sup> with a few exceptions.

4. The viscosity for the isotropic or fully anisotropic solutions at a given concentration increased with  $\bar{M}_n$ , whereas the viscosity for the solutions in the vicinity of the biphasic region showed a minimum with  $\bar{M}_n$ . The latter behavior is due to the phase transformation from biphasic to fully anisotropic phase. The slope of the shear viscosity at given shear rates vs.  $C\bar{M}_w$  was dependent on shear rate and the slope for the isotropic solutions appeared to be greater than that for fully anisotropic solutions.  $\Delta P_{\text{ent}}$  and  $\nu$  at a given concentration showed either a monotonical increase or a maximum or minimum with  $\bar{M}_n$ . This behavior depended on the phase of the solution and was not fully consistent with that of the viscosity.  $B$  for the isotropic solution increased with  $\bar{M}_n$  and  $B$ 's for both biphasic and fully anisotropic solutions were almost constant with  $\bar{M}_n$ . Apparently, the data of more wider MW range will be necessary.

### References

1. S. Suto, K. Obara, S. Nishitani, and M. Karasawa, *J. Polym. Sci., Polym. Phys. Ed.*, **24**, 1850 (1986).
2. S. Suto, K. Obara, and M. Karasawa, *Kobunshi Ronbunshu*, **43**, 321 (1986).
3. S. Suto, R. Ito, and M. Karasawa, *Polym. Commun.*, **26**, 335 (1985).
4. S. Suto, R. Ito, and M. Karasawa, *Sen-i Gakkaishi*, **42**, T-317 (1986).

5. S. Suto, M. Ohshiro, R. Ito, and M. Karasawa, *Nippon Reorogi Gakkaishi*, **14**, 87 (1986).
6. S. Suto, M. Ohshiro, R. Ito, and M. Karasawa, *Polymer*, **28**, 23 (1987).
7. S. Suto, M. Kudo, and M. Karasawa, *J. Appl. Polym. Sci.*, **31**, 1327 (1986).
8. S. Weller and W. A. Steiner, *J. Appl. Phys.*, **21**, 279 (1950).
9. (a) R. M. Barrer, J. A. Barrie, and J. Slater, *J. Polym. Sci.*, **23**, 315 (1957); (b) R. M. Barrer and J. A. Barrie, *J. Polym. Sci.*, **23**, 331 (1957).
10. V. Saxena and S. A. Stern, *J. Membr. Sci.*, **12**, 65 (1982).
11. (a) E. Casur and T. G. Smith, *J. Appl. Polym. Sci.*, **31**, 1425 (1986); (b) E. Casur and T. G. Smith, *J. Appl. Polym. Sci.*, **31**, 1441 (1986).
12. S. Suto, *J. Polym. Sci., Polym. Phys. Ed.*, **22**, 637 (1984).
13. S. Suto, H. Ise, and M. Karasawa, *J. Polym. Sci., Polym. Phys. Ed.*, **24**, 1515 (1986).
14. S. Suto, S. Kimura, and M. Karasawa, *J. Appl. Polym. Sci.*, **33**, 3019 (1987).
15. S. Suto, K. Oikawa, and M. Karasawa, *Polym. Commun.*, **27**, 262 (1986).
16. J. Bheda, J. F. Fellers, and J. L. White, *Colloid Polym. Sci.*, **258**, 1335 (1980).
17. W. R. Moore and A. M. Brown, *J. Appl. Chem.*, **8**, 363 (1958).
18. C. J. Clemett, *Anal. Chem.*, **45**, 186 (1973).
19. S. Suto, *J. Appl. Polym. Sci.*, to appear.
20. G. Kiss, *J. Rheol.*, **30**, 585 (1986).
21. S. N. Bhadani, S.-L. Tseng, and D. G. Gray, *Makromol. Chem.*, **184**, 1727 (1983).
22. M. A. Aden, E. Bianchi, A. Ciferri, G. Conio, and A. Tealdi, *Macromolecules*, **17**, 2010 (1984).
23. S. L. Wunder, S. Ramachandran, C. R. Gochanour, and M. Weinberg, *Macromolecules*, **19**, 1696 (1986).
24. S. P. Papkov, V. G. Kulichikhin, V. D. Kalmykova, and A. Ya. Malkin, *J. Polym. Sci., Polym. Phys. Ed.*, **12**, 1753 (1974).
25. W. W. Graessley, *Adv. Polym. Sci.*, **16**, 48 (1974).
26. K. F. Wissbrun, *J. Rheol.*, **25**, 619 (1981).
27. S. Onogi and T. Asada, *Rheology*, G. Astarita, G. Marrucci, and L. Nicolais, Eds., Plenum, New York, 1980, Vol. 1, p. 127.
28. B. Valenti and A. Ciferri, *J. Polym. Sci., Polym. Lett. Ed.*, **16**, 657 (1978).
29. G. Kiss and R. S. Porter, *J. Polym. Sci., Polym. Phys. Ed.*, **18**, 361 (1980).
30. W. George and P. Tucker, *Polym. Eng. Sci.*, **16**, 212 (1976).
31. Y. Onogi, J. L. White, and J. F. Fellers, *J. Non-Newt. Fluid Mech.*, **7**, 121 (1980).
32. T. Arai, H. Aoyama, and I. Suzuki, *Kogyo Kagaku Zashi*, **63**, 418 (1960).
33. M. Fujiyama and H. Awaya, *Zairyo*, **20**, 616 (1971).
34. J. J. Pena, G. M. Guzman, and A. Santamaria, *Polym. Eng. Sci.*, **21**, 307 (1981).
35. N. Minoshima, S. Kobayashi, M. Shimura, and Y. Kinoshita, *Kobunshi Kagaku*, **28**, 953 (1971).
36. D. V. Boger and R. Binnington, *Trans. Soc. Rheol.*, **21**, 515 (1977).
37. G. Pezzin, G. Ajroldi, and C. Garbuglio, *Rheol. Acta*, **8**, 304 (1969).
38. D. G. Baird, *J. Rheol.*, **24**, 465 (1980).
39. H. L. LaNieve and D. C. Bogue, *J. Appl. Polym. Sci.*, **12**, 353 (1968).
40. C. D. Han, *AIChE J.*, **17**, 1480 (1971).
41. L. Choplin and P. J. Carreau, *J. Non-Newt. Fluid Mech.*, **9**, 119 (1981).
42. A. Blumstein, O. Thomas, and S. Kumar, *J. Polym. Sci., Polym. Phys. Ed.*, **24**, 27 (1986).
43. M. G. Rogers, *J. Appl. Polym. Sci.*, **14**, 1679 (1970).
44. J. Vlachopoulos, M. Horie, and S. Lidorikis, *Trans. Soc. Rheol.*, **16**, 669 (1972).
45. R. Racin and D. C. Bogue, *J. Rheol.*, **23**, 263 (1979).

Received March 19, 1987

Accepted May 7, 1987